Published in final edited form as:
Curr Med Chem. 2011 September 1; 18(27): 4195–4205.

Molecular Imaging with Nucleic Acid Aptamers

Hao Hong[1], **Shreya Goel**[2], **Yin Zhang**[3], and **Weibo Cai**[1,3,4,*]

[1]Department of Radiology, University of Wisconsin - Madison, Madison, WI, USA

[2]Center of Nanotechnology, Indian Institute of Technology, Roorkee, India

[3]Department of Medical Physics, University of Wisconsin - Madison, Madison, WI, USA

[4]University of Wisconsin Carbone Cancer Center, Madison, WI, USA

Abstract

With many desirable properties such as ease of synthesis, small size, lack of immunogenicity, and versatile chemistry, aptamers represent a class of targeting ligands that possess tremendous potential in molecular imaging applications. Non-invasive imaging of various disease markers with aptamer-based probes has many potential clinical applications such as lesion detection, patient stratification, treatment monitoring, etc. In this review, we will summarize the current status of molecular imaging with aptamer-based probes. First, fluorescence imaging will be described which include both direct targeting and activatable probes. Next, we discuss molecular magnetic resonance imaging and targeted ultrasound investigations using aptamer-based agents. Radionuclide-based imaging techniques (single-photon emission computed tomography and positron emission tomography) will be summarized as well. In addition, aptamers have also been labeled with various tags for computed tomography, surface plasmon resonance, dark-field light scattering microscopy, transmission electron microscopy, and surface-enhanced Raman spectroscopy imaging. Among all molecular imaging modalities, no single modality is perfect and sufficient to obtain all the necessary information for a particular question. Thus, a multimodality probe has also been constructed for concurrent fluorescence, gamma camera, and magnetic resonance imaging in vivo. Although the future of aptamer-based molecular imaging is becoming increasingly bright and many proof-of-principle studies have already been reported, much future effort needs to be directed towards the development of clinically translatable aptamer-based imaging agents which will eventually benefit patients.

Keywords

Aptamers; molecular imaging; cancer; positron emission tomography; DNA/RNA; fluorescence; personalized medicine

INTRODUCTION

Aptamers, single-stranded DNA or RNA sequences typically generated through the process termed “Systematic Evolution of Ligands by EXponential enrichment (SELEX)” [1,2], have recently emerged as a promising class of ligands with superb potential for diagnostic and therapeutic applications [3]. Alternatively, a MonoLEX method has also been reported which comprises a single affinity chromatography step, followed by physical segmentation of the affinity resin and a polymerase chain reaction (PCR) amplification step of bound

Requests for reprints: Weibo Cai, PhD, Departments of Radiology and Medical Physics, University of Wisconsin - Madison, Room 7137, 1111 Highland Ave, Madison, WI 53705-2275, USA, wcai@uwhealth.org; Phone: 608-262-1749; Fax: 608- 265-0614.

aptamers [4]. Aptamers (with molecular weight of 5–40 kDa) can fold into well-defined 3D structures and bind to their target molecules with high affinity and specificity. To date, aptamers have been selected against a wide range of targets such as proteins, phospholipids, sugars, nucleic acids, whole cells, among others [3]. Since wild-type RNA and DNA molecules can be easily degraded by nucleases, various strategies have been adopted to synthesize aptamers with enhanced in vitro/in vivo stability, such as the use of polyethylene glycol (PEG) conjugation [5], unnatural internucleotide linkages [6], chemically modified oligonucleotides [7–9], Spiegelmers (where the sugars are enantiomers of wild-type nucleic acid sugars) [10,11], among many others [3]. In the two decades since aptamers were first selected through SELEX, Pegaptanib (Pfizer/Eyetech), an aptamer that binds to human vascular endothelial growth factor (VEGF), has been approved by the United States Food and Drug Administration (FDA) for clinical use in treating age-related macular degeneration (AMD) [12]. In addition, a variety of aptamers against other molecular targets are currently under clinical investigation [3].

The field of molecular imaging, “the visualization, characterization and measurement of biological processes at the molecular and cellular levels in humans and other living systems” [13], has expanded tremendously over the last decade. Commonly used molecular imaging modalities include molecular magnetic resonance imaging (MRI), bioluminescence, fluorescence, targeted ultrasound, single photon emission computed tomography (SPECT), and positron emission tomography (PET) [14]. Capable of giving whole body readouts in intact systems which is much more relevant and reliable than in vitro/ex vivo assays, non-invasive molecular imaging of molecular markers of various diseases can allow for much earlier diagnosis, earlier treatment, and better prognosis that will eventually lead to personalized medicine [14,15]. Continued development and wider availability of scanners dedicated to small animal imaging studies, which can provide a similar in vivo imaging capability in mice, primates, and humans, can enable smooth transfer of knowledge and molecular measurements between species thereby facilitating clinical translation of novel imaging agents and/or techniques.

With many advantages over other commonly used targeting ligands (e.g. antibodies) such as easier synthesis, lower batch-to-batch variability, better thermal stability, smaller size, lower immunogenicity, more versatile chemistry, among others [3], aptamers possess enormous potential in molecular imaging applications. In this review, we will summarize the current status of molecular imaging with aptamer-based agents.

OPTICAL IMAGING

Optical imaging, which typically includes bioluminescence and fluorescence, is a relatively low-cost method suitable primarily for small animal studies [16,17]. Fluorescence imaging with aptamer-based agents has been well documented in the literature. Since many aptamers have relatively weak binding affinities to their targets, in many cases aptamers were conjugated to various nanoparticles (NPs) to improve the binding avidity and targeting efficacy. For example, gold-silver nanorods (NRs) have been used as a nanoplatform for multivalent binding of multiple aptamers to enhance both the signal intensity and binding affinity for cancer cell recognition [18]. Up to 80 fluorophore-labeled aptamers could be attached on each NR, resulting in enhanced fluorescence signal. Generally speaking, aptamer-based optical imaging can be divided into two categories: direct targeting and activatable probes.

Direct Targeting with Aptamers

A number of molecular targets have been explored for aptamer-based optical imaging. Integrin $\alpha_v\beta_3$ is a cell adhesion molecule involved in a wide variety of physiological

processes such as cell growth/migration, tumor invasion/metastasis, angiogenesis, and wound healing [19,20]. In one study, an RNA aptamer that binds to recombinant integrin $\alpha_v\beta_3$ was labeled with Cy5 and tested for its ability to bind to endogenous integrin $\alpha_v\beta_3$ on cell surface, as well as to subsequently affect cellular responses [21]. In another report, an aptamer that binds to angiogenin (a potent angiogenic factor which plays an important role in tumor angiogenesis [22,23]) with high specificity was employed to study the cellular internalization of angiogenin [24]. Dynamic confocal imaging in cell culture indicated that the aptamer-angiogenin conjugate was quickly internalized, which provided the first evidence that a fluorophore-labeled aptamer could be used for visualizing the spatiotemporal process of protein internalization in real time. Besides these two angiogenesis-related proteins, aptamer-based fluorescence imaging has been explored for a variety of other molecular targets.

Prostate-specific membrane antigen (PSMA)—PSMA, a 100 kDa type II transmembrane glycoprotein, is one of the best characterized targets in oncology [25]. PSMA expression levels have been shown to exhibit a positive correlation with increased tumor progression, development of castration resistance, and/or resistance to hormone-based therapies [26]. In one study, Cy5-conjugated polylactide (Cy5-PLA) NPs were synthesized [27]. The Cy5-PLA NPs were subsequently conjugated to the A10 RNA aptamer, which recognizes the extracellular domain of PSMA [28]. In vitro, the Cy5-PLA NP-A10 conjugate was found to only bind to and get internalized by PSMA-positive cells but not PSMA-negative cells [27]. Interestingly, only the Cy5-PLA NPs were tested in vivo in normal mice but not the PSMA-targeting conjugate.

Quantum dots (QDs) are inorganic fluorescent semiconductor nanoparticles with many desirable properties for imaging applications such as high quantum yields, high molar extinction coefficients, strong resistance to photobleaching and chemical degradation, narrow emission spectra, large effective Stokes shifts, among others [17,29]. PSMA-specific aptamers have been conjugated to QDs for imaging of PSMA-positive cells [30]. The specific binding capability and synthetic accessibility of aptamers, when combined with photostability and small sizes of QDs, offered a powerful and general tool for cellular imaging.

Fluorescent resonance energy transfer (FRET) is a commonly used technique for imaging biologically interacting molecules in cells [31,32]. A Bi-FRET QD-Apt-Dox conjugate (Apt and Dox denote aptamer and doxorubicin, respectively) was constructed as both an imaging agent and a drug delivery vehicle (Fig. (1)) [33]. The A10 RNA aptamer was attached covalently to the QD surface, while Dox was intercalated in the double-stranded stem region of the A10 aptamer. Since the fluorescence of QD was quenched by the absorbance of Dox and the fluorescence of Dox was quenched by the A10 aptamer, this QD-Apt-Dox conjugate is initially in the fluorescence “OFF” state. After the conjugate was taken up by PSMA-positive cancer cells, Dox was gradually released which led to a recovery of the fluorescence signal from QD and Dox (i.e. the “ON” state). Therefore, this multifunctional QD-Apt-Dox conjugate can be used for not only drug delivery to targeted cells, but also for monitoring the delivery/release of the drug and concurrently imaging the target cells. Cytotoxicity of QD-Apt-Dox was found to be significantly higher in PSMA-positive cells than PSMA-negative cells.

Nucleolin—An aptamer called AS1411 was selected against nucleolin, a phosphoprotein involved in the synthesis and maturation of ribosomes [34,35]. FRET was applied to image the colocalization of two proteins (i.e. nucleolin and integrin $\alpha_v\beta_3$) in the membrane of cancer cells [36]. AS1411 was labeled with a fluorescent dye Cy3 (termed “Cy3-AS1411”) while arginine-glycine-aspartic acid (RGD) peptides, which are potent antagonists of

integrin $\alpha_v\beta_3$ [37,38], were conjugated to QDs (termed "QD-RGD") [36]. FRET activities between Cy3-AS1411 and QD-RGD in HeLa human cervical cancer cells revealed that both nucleolin and integrin $\alpha_v\beta_3$ were highly expressed. In addition, these studies also provided information on the geographical colocalization of the two proteins, which may be useful in determining the molecular/cellular functions of certain genes involved in cancer and/or other diseases in the future. In a related study, multiplexed fluorescence imaging of two different QDs (conjugated with AS1411 and RGD peptides, respectively) in cancer cells was reported [39]. Simultaneous imaging of cellular distribution of nucleolin and integrin $\alpha_v\beta_3$ in cancer cells was achieved, demonstrating the feasibility of concurrent visualization of multiple cancer markers using QDs conjugated with small molecules such as aptamers or peptides.

Recently, chemical modification of AS1411 with Cy3 labeled 5-(N-benzylcarboxyamide)-2'-deoxyuridine (5-BzdU) was performed [40]. Forty-seven modified AS1411 aptamers were synthesized by randomly substituting 1–12 thymidines in AS1411 with Cy3-labeled 5-BzdU. Through fluorescence and confocal microscopy studies, several compounds were identified as possessing significantly increased targeting affinity to cancer cells but not normal cells. This study suggested that the position and number of substituents in AS1411 are critical parameters in improving the aptamer function, and chemical modification of existing aptamers may suffice in enhancing their binding affinity/specificity without the need to perform additional SELEX procedures.

Other Targets—A wide variety of other molecular targets have been investigated for aptamer-based imaging. Mucin 1 (MUC1), a protein expressed on most cancers of glandular epithelial origin, is a promising target for therapeutic interventions in these cancers [41,42]. One report has described the design of a tumor-targeted, pH-responsive conjugate for chemotherapy of ovarian cancer [43]. QDs were conjugated with DNA aptamers specific for MUC1 and Dox was attached to the QD via a pH-sensitive hydrazone bond, which can allow for drug release under the acidic environment inside cancer cells. Confocal microscopy and in vivo imaging studies confirmed higher cytotoxicity of the MUC1-targeted conjugate to multidrug-resistant cancer cells, as well as preferential accumulation in ovarian tumors, as compared to unconjugated Dox.

A QD-Apt complex was synthesized by linking a streptavidin-modified QD to a biotin-conjugated aptamer via the biotin-streptavidin interaction [44]. The conjugate was shown to not affect the growth and viability of targeted cells, thereby demonstrating its biocompatibility and suitability for live cell imaging. In another study, a QD-A22 conjugate was constructed for virus visualization, where A22 is an aptamer that binds to hemagglutinin of the influenza A virus [45]. Recently, sensitive colorimetric detection of biomolecules was achieved, which utilized aptamers immobilized on a gold NP composite film [46].

Aptamer-conjugated NPs have been investigated for the collection and detection of cancer cells. For example, aptamer-conjugated magnetic NPs were used for selectively targeted cell extraction, whereas aptamer-conjugated fluorescent NPs were employed for sensitive detection of cells [47]. In addition, a single-molecule imaging approach has been developed for investigating the functional heterogeneity of RNA aptamers [48], which may be useful in elucidating the relationship between biopolymer information and function.

Recently, in vivo fluorescence imaging of tumors using a Cy5-labeled aptamer (TD05, which was generated by cell-SELEX [49]) was carried out in a xenograft model [50]. It was demonstrated that this conjugate could effectively recognize tumors with high sensitivity and specificity. In an interesting report, a fluorogenic cyanine dye, which has low fluorescence quantum yield, exhibited an 80-fold enhanced fluorescence in glycerol solution in the presence of double-stranded DNA [51]. An RNA aptamer selected for binding to this

dye also resulted in a 60-fold fluorescence enhancement. It was suggested that such dye-aptamer pairs may be incorporated into the future design of fluorescent sensors.

Aptamer-Based Activatable Probes

Different from directly targeted probes where aptamers were conjugated to dyes, QDs, or other NPs for fluorescence imaging applications, activatable probes can change their optical properties after biological interactions such as enzyme cleavage [52,53] or nucleic acid complementation [54,55]. Typically, a fluorescently labeled substrate is designed to be maximally quenched by a quencher (in some cases the fluorescent dye itself) in close proximity because of FRET [56,57]. Upon enzyme cleavage or nucleic acid complementation, the fluorophore and the quencher are separated which results in enhanced fluorescence signal.

Such strategy was adopted for the imaging of myotonic dystrophy kinase-related Cdc42-binding kinase (MRCK), an important signal transduction protein which is a downstream effector of Cdc42 [58]. The aptamer that binds to MRCK was modified into an activatable probe by adding nucleotides on the 5’ end, which are complementary to its 3’ end, thereby forming a “molecular beacon” with a fluorophore-quencher pair at the 5’ and 3’ ends, respectively. This conjugate is hairpin-shaped in the absence of MRCK. When MRCK is present, the MRCK-aptamer complex forms, leading to a change in fluorescence signal that is detectable in cell-based studies. In a recent report, an activatable probe targeting membrane proteins on cancer cells was synthesized and investigated for tumor imaging in mice (Fig. (2)) [59]. In vivo studies confirmed the presence of activated fluorescence signals in the targeted tumor. Comparing to a conventional “always-on” probe, the activatable probe could substantially minimize the background signal originating from non-target tissues, thereby giving significantly enhanced image contrast.

MAGNETIC RESONANCE IMAGING

MRI detects the interaction of protons (or certain other nuclei) with each other and with the surrounding molecules in a tissue of interest. Different tissues have different relaxation times that result in endogenous contrast in MRI [60]. Exogenous contrast agents can further enhance this by selectively shortening either the T1 (longitudinal) or T2 (transverse) relaxation time. Traditionally, Gd^{3+}-chelates have been used to enhance the T1 contrast [61] and iron oxide NPs have been used to increase the T2 contrast [62]. The progress in activatable fluorescent probes has also inspired the development of activatable probes for MRI.

A “turn-on” MRI contrast agent was designed based on a SPIO-aptamer conjugate, where SPIO denotes superparamagnetic iron oxide NPs and an aptamer against adenosine was used [63]. Target-induced disassembly of clustered NPs in the presence of adenosine led to an increase in T2, which was detectable in MRI. Recently, the same group reported another MRI contrast agent for sensing of adenosine [64]. Direct modification of SPIOs with a biomolecule (i.e. hemin), as well as sequence-specific assembly of the modified SPIO via an aptamer-small molecule interaction, was reported [65]. However, the SPIO-based agents were not tested for MRI applications. In another study, a MRI contrast agent based on iron oxide NPs and aptamers was constructed for the detection of human α-thrombin protein, where addition of thrombin resulted in aggregation of the NPs thereby reducing the T2 relaxation time [66]. This agent was demonstrated to be thrombin specific with sensitivity in the nanomolar range (Fig. (3)).

Mesenchymal stem cells (MSCs) represent a promising cell source for cellular cardiomyoplasty [67,68]. Aptamer-based selection of MSCs was employed to provide

"ready to transplant" cells directly after isolation [69]. Tracking of newly isolated and freshly transplanted MSCs with MRI was carried out in a porcine heart perfusion model, after aptamer-based isolation and appropriate labeling of the cells. This study demonstrated that isolating MSCs by MSC-specific aptamers linked to magnetic NPs is feasible and effective, which combines specific separation and labeling into a "one stop shop" strategy.

A SPIO-based agent was developed for combined prostate cancer imaging and therapy applications, where the A10 aptamer was attached to thermally cross-linked SPIO, which could act as both a MRI contrast agent and a carrier for Dox [70]. The conjugate was demonstrated to be capable of detecting prostate cancer cells with high sensitivity and specificity, corroborated by another recent study [71]. In an intriguing report, aptamer-conjugated magnetic NPs were developed as "nanosurgeons" for selective removal of target cells by controlling the conjugate with an externally applied rotational magnetic field [72]. It was suggested that these "nanosurgeons" may become a useful tool for selective surgery and cell manipulation studies.

TARGETED ULTRASOUND

Ultrasound is the most commonly used clinical imaging modality because of its safety, low cost, ease of use, and wide availability [73,74]. However, it is not until recently that ultrasound studies using aptamers as the targeting ligands were reported. An aptamer was covalently conjugated to nanobubbles for targeted ultrasound imaging [75]. Upon optimization of the conjugation chemistry, various experiments were carried out to evaluate the performance and consistency of the prepared nanobubbles, such as size distribution, conjugation efficiency, etc. Ex vivo ultrasound imaging was also performed and compared with optical imaging. It was suggested that aptamer-conjugated nanobubbles can be useful probes for molecular imaging, with potential applications in dose quantification of targeted ultrasound-triggered drug delivery. In another report, a computational modeling approach was adopted to maximize aptamer-microbubble binding to the target molecules [76]. This model gave useful insights into the key parameters (e.g. microbubble size, drag forces, number/type of targeting ligands, etc.) for stable microbubble binding, which may allow a flexible, prospective design and optimization of microbubbles to facilitate clinical translation of ultrasound-based molecular imaging.

SPECT AND PET IMAGING

Radionuclide-based imaging techniques (i.e. SPECT and PET) have much higher clinical potential than the other molecular imaging modalities, since SPECT and PET have superb tissue penetration capability and they are highly quantitative [14,52]. Labeling of single-stranded oligonucleotides with radioisotopes (e.g. ^{99m}Tc, ^{111}In, ^{125}I, etc. for SPECT or ^{11}C, ^{18}F, ^{76}Br, ^{64}Cu. etc. for PET) can result in valuable radiopharmaceuticals with promising applications [77–79]. However, oligonucleotides are intrinsically poor pharmaceuticals because of their low stability, poor membrane passage, and various undesirable and sometimes unpredictable side effects. Aptamers are a promising class of oligonucleotides that is well suited for imaging applications.

The source of SPECT images is gamma ray emission [80]. The gamma camera can be used in planar imaging to obtain 2D images, or in SPECT imaging to obtain 3D images. In one early study, in vivo imaging of inflammation in a rat model was achieved using ^{99m}Tc-labeled aptamers [81]. The enzyme elastase, which binds to the surface of activated neutrophils [82], was chosen as the target. An aptamer inhibitor of elastase, isolated in a previous report [83], was tested for imaging applications. Higher target-to-background ratio than antibody-based agents was observed.

Almost a decade later, another aptamer (termed "TTA1") which binds to tenascin-C (an extracellular matrix protein overexpressed in many solid tumors [84,85]) was labeled with ^{99m}Tc for tumor imaging (Fig. (4)) [86]. Biodistribution and imaging studies of ^{99m}Tc-labeled TTA1 were performed in several xenograft models, which exhibited rapid blood clearance (with a circulation half-life of < 2 min) and tumor penetration. The durable tumor retention in combination with fast blood clearance yielded an excellent tumor-to-blood ratio, and various tumors were clearly visualized by planar scintigraphy. Besides ^{99m}Tc, TTA1 was also labeled with a fluorescent dye for optical imaging applications. Intravenous injection of the fluorescently labeled TTA1 into mice resulted in bright perivascular fluorescence in a xenografted tumor within 10 minutes post-injection, with the fluorescence signal gradually diffusing throughout the tumor over time.

Subsequently, aptamers that bind to MUC1 were labeled with ^{99m}Tc through a cyclen-based ligand, which has a sulfur-containing arm that increases the stability of the ligand-metal complex [87]. In this study, a series of aptamers targeting MUC1 were selected through SELEX and chemically modified to improve the in vivo stability. Both monomeric and tetrameric aptamer conjugates (based on monovalent and tetravalent bifunctional chelators, respectively) were synthesized and investigated in vitro and in vivo, with the tetrameric aptamers exhibiting superior tumor retention and pharmacokinetic properties than the monomers. However, it was concluded that the ligands were not ideal for metal binding, and additional ligands would need to be explored in the future. In a follow-up report, these aptamers were conjugated to MAG2 (a commonly used chelator for ^{99m}Tc [88]) and labeled with ^{99m}Tc for imaging of breast cancer [89]. Although efficient radiolabeling of the aptamers was achieved, the tumor uptake was very low while radioactivity in the intestines was high.

PET, a nuclear medicine imaging technique which produces a 3D image or map of functional processes in the body, was first developed in the mid-1970s [90,91]. PET has higher sensitivity than SPECT [92]. With the continuous developmental effort, state-of-the-art small animal PET scanners can now have spatial resolution (< 1 mm) comparable to SPECT and they are also becoming increasingly widely available [93,94]. To the best of our knowledge, there is only one report on labeling aptamers for potential PET imaging applications [95]. In this study, the choice of chelators and radiolabeling parameters such as pH and temperature were investigated for the development of ^{64}Cu-labeled RNA aptamers for potential PET imaging. However, no in vivo studies were reported.

OTHER IMAGING TECHNIQUES

Besides the abovementioned studies where aptamers were labeled with various tags for molecular imaging applications with each modality, aptamers have also been explored for several other imaging techniques such as computed tomography (CT), surface plasmon resonance (SPR), dark-field light scattering microscopy and transmission electron microscopy (TEM) [96], as well as surface-enhanced Raman spectroscopy (SERS) imaging [97].

Computed Tomography

CT is a medical imaging method where digital geometry processing is used to generate a 3D image of the internals of an object from a large series of 2D X-ray images taken around a single axis of rotation [98]. Current CT contrast agents are typically iodine-based molecules, which exhibit non-specific distribution and rapid clearance [99,100]. Iodinated NPs and polymer-coated Bi_2S_3 NPs have also been investigated as CT contrast agents [101–104].

Recently, a drug-loaded aptamer-gold NP bioconjugate was reported for combined CT imaging and therapy of prostate cancer [105]. By functionalizing the surface of gold NPs with an aptamer that recognizes PSMA, molecular CT imaging was achieved in cell culture, where the PSMA-targeted NPs exhibited several fold higher CT intensity in the targeted cells when compared with control cells. In addition, Dox-loaded NPs were also significantly more potent against the targeted cells than control cells. Although detectable by CT, the major role of gold NP in this conjugate was to serve as a drug-loading platform rather than an imaging contrast agent. The poor sensitivity of CT severely limits the clinical potential of molecular CT imaging using a targeted contrast agent.

Surface Plasmon Resonance

Surface plasmons are surface electromagnetic waves that propagate in a direction parallel to the metal/dielectric (or metal/vacuum) interface. Since the wave is at the boundary of the metal and the external medium (e.g. air or water), these oscillations are very sensitive to changes such as adsorption of molecules onto the metal surface [106,107]. By patterning the surface with different biopolymers and using adequate optics and imaging sensors, SPR images can be generated based on the amount of adsorbed molecules.

RNA microarrays created on chemically modified gold surfaces were employed for SPR measurement of DNA-RNA hybridization and RNA aptamer-protein binding [108]. SPR imaging enabled identification of the best aptamer to factor IXa from among those previously selected via SELEX. More importantly, single-base variations from this sequence were shown to completely destroy the aptamer-factor IXa interaction. Using a similar strategy, the adsorption of proteins onto a RNA microarray was detected by the formation of a surface aptamer-protein-antibody complex (Fig. (5)) [109]. A combination of RNA aptamers and antibodies was used to detect protein biomarkers at picomolar concentrations, with a sensitivity level comparable to those achieved with conventional ELISA assays. However, this technique requires both an RNA aptamer and an antibody that bind to different sites on the target protein, which is quite challenging in many scenarios. Recently, the same group also reported rapid microarray SPR detection of DNA and proteins in microliter volumes using microfluidic chips [110]. A detection limit of 10 femtomolar or 30 zeptomoles was achieved.

In another report, SPR imaging was used for affinity analysis of aptamer-protein interactions with microfluidic chips [111]. Such aptamer affinity screening by SPR imaging was suggested to be advantageous over other competing methods because it does not require labeling, can be used in real-time, and is potentially high-throughput. In addition, the ability to provide both qualitative and quantitative results on a multichannel chip makes SPR imaging a powerful tool for studying biological interactions in a multiplexed format. Recently, aptamer-based biochips for label-free detection of plant virus coat proteins by SPR imaging was also reported [112].

MULTIMODALITY IMAGING

Among all molecular imaging techniques, no single modality is perfect and sufficient to obtain all the necessary information for a particular question [14]. For example, it is difficult to accurately quantify fluorescence signal in living subjects, particularly in deep tissues; MRI has high resolution yet it suffers from low sensitivity; Radionuclide-based imaging techniques have very high sensitivity but have relatively poor spatial resolution. Combination of multiple molecular imaging modalities can offer synergistic advantages over any modality alone. Multimodality imaging using a small molecule-based probe is very challenging due to the limited number of conjugation sites and the potential interference

with its target binding affinity. On the other hand, NPs have large surface areas where multiple functional moieties can be incorporated for multimodality molecular imaging.

A multimodality probe was constructed for concurrent fluorescence, gamma camera, and magnetic resonance imaging in vivo (Fig. (6)) [113]. A cobalt-ferrite NP coated with rhodamine was modified with the AS1411 aptamer, which was then conjugated to a chelating agent and further labeled with ^{67}Ga (termed "MFR-AS1411"). Cellular distribution of nucleolin was evaluated by fluorescence confocal microscopy with MFR-AS1411, which exhibited specific fluorescence signals in nucleolin-expressing cancer cells. In vivo, MFR-AS1411 specifically targeted the cancer cells as evidenced by both gamma camera imaging and dark T2 signals inside the tumor region of mice injected with MFR-AS1411, suggesting that this agent may be useful for multimodality imaging of disease, theranostics, and potentially also the study of cellular metabolism.

CONCLUSIONS AND FUTURE PERSPECTIVES

Significant progress has been made over the last two decades since SELEX was first reported [1,2]. With many desirable properties, aptamers represent a class of targeting ligands that possess tremendous potential in both imaging and therapeutic applications [3,114–116]. As therapeutics, one aptamer (i.e. Pegaptanib) has been approved by the FDA and many others are in late phase clinical trials [3,12]. As imaging agents, aptamers have been surprisingly understudied. Nonetheless, molecular imaging with aptamer-based agents has been achieved with many imaging modalities (Table 1). Non-invasive molecular imaging of various disease markers with aptamer-based probes has potential clinical applications in many aspects: lesion detection, patient stratification, new drug development/validation, treatment monitoring, dose optimization, among others [15,117,118]. Much further effort should be directed towards the development of clinically translatable aptamer-based imaging agents, which can help paving the road to 21st century personalized medicine.

Each imaging modality has its advantages and disadvantages in terms of sensitivity, spatial resolution, tissue penetration, clinical potential, etc. [14]. Optical imaging is mostly applicable to preclinical studies, where light penetration is not a major issue, while ultrasound, MRI, SPECT and/or PET are more clinically relevant. Optical imaging in the near-infrared (700–900 nm) region can offer better light penetration and will find many applications in the clinic such as breast cancer imaging, intraoperative imaging, or imaging tumors that are accessible by endoscopy or near the skin surface [17,119]. Combination of various imaging modalities can give complementary information, as illustrated in one study mentioned above [113]. More aptamer-based multimodality imaging probes should be developed in the future. Strategies that combine radionuclide-based imaging (very sensitive and highly quantitative) and non-radionuclide based approaches, e.g. optical imaging which can significantly facilitate ex vivo validation of the in vivo data [120,121] and/or MRI which can provide anatomical information with high resolution [122,123], are of particular interest. For example, one clinical scenario where a PET/optical agent is particularly useful is that an initial whole body PET scan can be carried out to identify the location of tumor(s), and the optical component can subsequently help pinpointing the tumor position during surgical resection.

To date, researchers have identified high-affinity aptamers that target a broad array of protein families including cytokines, proteases, kinases, cell-surface receptors, cell-adhesion molecules, among others [3,114–116]. Since aptamers can be selected against most protein targets, the possible applications of aptamer-based molecular imaging range far and wide. One disadvantage of aptamers is the hard-to-predict and poorly understood

pharmacokinetics, toxicity, and certain other properties upon systemic delivery. Although aptamers are unlikely to elicit an immune response, at least at the antibody level, the safety profile of each individual aptamer (conjugate) must be examined carefully. However, this aspect is not of major concern for imaging applications since only trace amount of aptamers will be needed, in contrast to the large doses necessary for therapeutic purposes.

One major advantage of aptamers is that they are quite specific and have high binding affinity, which makes them suitable for drug delivery and internal radiotherapy applications. Besides the imaging agents described in this review, aptamers can also be used to deliver other anti-cancer agents such as therapeutic radioisotopes (e.g. α-particle emitters such as ^{211}At and ^{225}Ac, β-particle emitters such as ^{90}Y, ^{67}Cu, ^{131}I, ^{177}Lu, ^{186}Re, and ^{188}Re, and Auger electron emitters such as ^{111}In and ^{125}I) [124]. With more and more academic groups and companies getting involved in aptamer-based research after the earliest aptamer intellectual property expires [125], the development of aptamer-based imaging agents will speed up and aptamers will find their own niches in molecular imaging and revolutionize cancer diagnosis and clinical patient management. The future of aptamer-based molecular imaging is becoming increasingly bright since many proof-of-principle studies have already been reported, yet much remains to be done before aptamer-based imaging agents can reach clinical trials and eventually the day-to-day management of patients.

Acknowledgments

The authors acknowledge financial support from the University of Wisconsin Carbone Cancer Center, NCRR 1UL1RR025011, and a DOD PCRP IDEA Award.

REFERENCES

1. Ellington AD, Szostak JW. In vitro selection of RNA molecules that bind specific ligands. Nature. 1990; 346:818–822. [PubMed: 1697402]
2. Tuerk C, Gold L. Systematic evolution of ligands by exponential enrichment: RNA ligands to bacteriophage T4 DNA polymerase. Science. 1990; 249:505–510. [PubMed: 2200121]
3. Keefe AD, Pai S, Ellington A. Aptamers as therapeutics. Nat. Rev. Drug Discov. 2010; 9:537–550. [PubMed: 20592747]
4. Nitsche A, Kurth A, Dunkhorst A, Panke O, Sielaff H, Junge W, Muth D, Scheller F, Stocklein W, Dahmen C, Pauli G, Kage A. One-step selection of Vaccinia virus-binding DNA aptamers by MonoLEX. BMC Biotechnol. 2007; 7:48. [PubMed: 17697378]
5. Takafuji Y, Jo JI, Tabata Y. Simple PEG modification of DNA aptamer based on copper ion coordination for tumor targeting. J. Biomater. Sci. Polym. Ed. 2010 Epub.
6. King DJ, Safar JG, Legname G, Prusiner SB. Thioaptamer interactions with prion proteins: sequence-specific and non-specific binding sites. J. Mol. Biol. 2007; 369:1001–1014. [PubMed: 17481659]
7. Lin Y, Nieuwlandt D, Magallanez A, Feistner B, Jayasena SD. High-affinity and specific recognition of human thyroid stimulating hormone (hTSH) by in vitro-selected 2'-amino-modified RNA. Nucleic Acids Res. 1996; 24:3407–3414. [PubMed: 8811096]
8. Rusconi CP, Scardino E, Layzer J, Pitoc GA, Ortel TL, Monroe D, Sullenger BA. RNA aptamers as reversible antagonists of coagulation factor IXa. Nature. 2002; 419:90–94. [PubMed: 12214238]
9. Pagratis NC, Bell C, Chang YF, Jennings S, Fitzwater T, Jellinek D, Dang C. Potent 2'-amino-, and 2'-fluoro-2'-deoxyribonucleotide RNA inhibitors of keratinocyte growth factor. Nat. Biotechnol. 1997; 15:68–73. [PubMed: 9035109]
10. Eulberg D, Klussmann S. Spiegelmers: biostable aptamers. Chembiochem. 2003; 4:979–983. [PubMed: 14523914]
11. Vater A, Klussmann S. Toward third-generation aptamers: Spiegelmers and their therapeutic prospects. Curr. Opin. Drug Discov. Devel. 2003; 6:253–261.

12. Ng EW, Shima DT, Calias P, Cunningham ET Jr, Guyer DR, Adamis AP. Pegaptanib, a targeted anti-VEGF aptamer for ocular vascular disease. Nat. Rev. Drug Discov. 2006; 5:123–132. [PubMed: 16518379]
13. Mankoff DA. A definition of molecular imaging. J. Nucl. Med. 2007; 48:18N–21N.
14. Massoud TF, Gambhir SS. Molecular imaging in living subjects: seeing fundamental biological processes in a new light. Genes Dev. 2003; 17:545–580. [PubMed: 12629038]
15. Weissleder R, Pittet MJ. Imaging in the era of molecular oncology. Nature. 2008; 452:580–589. [PubMed: 18385732]
16. Sokolov K, Aaron J, Hsu B, Nida D, Gillenwater A, Follen M, MacAulay C, Adler-Storthz K, Korgel B, Descour M, Pasqualini R, Arap W, Lam W, Richards-Kortum R. Optical systems for in vivo molecular imaging of cancer. Technol. Cancer Res. Treat. 2003; 2:491–504. [PubMed: 14640761]
17. Cai W, Hsu AR, Li ZB, Chen X. Are quantum dots ready for *in vivo* imaging in human subjects? Nanoscale Res. Lett. 2007; 2:265–281. [PubMed: 21394238]
18. Huang YF, Chang HT, Tan W. Cancer cell targeting using multiple aptamers conjugated on nanorods. Anal. Chem. 2008; 80:567–572. [PubMed: 18166023]
19. Hood JD, Cheresh DA. Role of integrins in cell invasion and migration. Nat. Rev. Cancer. 2002; 2:91–100. [PubMed: 12635172]
20. Cai W, Niu G, Chen X. Imaging of integrins as biomarkers for tumor angiogenesis. Curr. Pharm. Des. 2008; 14:2943–2973. [PubMed: 18991712]
21. Mi J, Zhang X, Giangrande PH, McNamara JO 2nd, Nimjee SM, Sarraf-Yazdi S, Sullenger BA, Clary BM. Targeted inhibition of $\alpha_v\beta_3$ integrin with an RNA aptamer impairs endothelial cell growth and survival. Biochem. Biophys. Res. Commun. 2005; 338:956–963. [PubMed: 16256939]
22. Badet J. Angiogenin, a potent mediator of angiogenesis. Biological, biochemical and structural properties. Pathol. Biol. (Paris). 1999; 47:345–351. [PubMed: 10372403]
23. Tello-Montoliu A, Patel JV, Lip GY. Angiogenin: a review of the pathophysiology and potential clinical applications. J. Thromb. Haemost. 2006; 4:1864–1874. [PubMed: 16961595]
24. Li W, Yang X, Wang K, Tan W, He Y, Guo Q, Tang H, Liu J. Real-time imaging of protein internalization using aptamer conjugates. Anal. Chem. 2008; 80:5002–5008. [PubMed: 18533682]
25. Olson WC, Heston WD, Rajasekaran AK. Clinical trials of cancer therapies targeting prostate-specific membrane antigen. Rev. Recent Clin. Trials. 2007; 2:182–190. [PubMed: 18474004]
26. Ghosh A, Heston WD. Tumor target prostate specific membrane antigen (PSMA) and its regulation in prostate cancer. J. Cell Biochem. 2004; 91:528–539. [PubMed: 14755683]
27. Tong R, Coyle VJ, Tang L, Barger AM, Fan TM, Cheng J. Polylactide nanoparticles containing stably incorporated cyanine dyes for in vitro and in vivo imaging applications. Microsc. Res. Tech. 2010; 73:901–909. [PubMed: 20146347]
28. Lupold SE, Hicke BJ, Lin Y, Coffey DS. Identification and characterization of nuclease-stabilized RNA molecules that bind human prostate cancer cells via the prostate-specific membrane antigen. Cancer Res. 2002; 62:4029–4033. [PubMed: 12124337]
29. Li ZB, Cai W, Chen X. Semiconductor quantum dots for *in vivo* imaging. J. Nanosci. Nanotechnol. 2007; 7:2567–2581. [PubMed: 17685272]
30. Chu TC, Shieh F, Lavery LA, Levy M, Richards-Kortum R, Korgel BA, Ellington AD. Labeling tumor cells with fluorescent nanocrystal-aptamer bioconjugates. Biosens. Bioelectron. 2006; 21:1859–1866. [PubMed: 16495043]
31. Jares-Erijman EA, Jovin TM. FRET imaging. Nat. Biotechnol. 2003; 21:1387–1395. [PubMed: 14595367]
32. Medintz IL, Clapp AR, Mattoussi H, Goldman ER, Fisher B, Mauro JM. Self-assembled nanoscale biosensors based on quantum dot FRET donors. Nat. Mater. 2003; 2:630–638. [PubMed: 12942071]
33. Bagalkot V, Zhang L, Levy-Nissenbaum E, Jon S, Kantoff PW, Langer R, Farokhzad OC. Quantum dot-aptamer conjugates for synchronous cancer imaging, therapy, and sensing of drug delivery based on bi-fluorescence resonance energy transfer. Nano Lett. 2007; 7:3065–3070. [PubMed: 17854227]

34. Soundararajan S, Chen W, Spicer EK, Courtenay-Luck N, Fernandes DJ. The nucleolin targeting aptamer AS1411 destabilizes Bcl-2 messenger RNA in human breast cancer cells. Cancer Res. 2008; 68:2358–2365. [PubMed: 18381443]
35. Teng Y, Girvan AC, Casson LK, Pierce WM Jr, Qian M, Thomas SD, Bates PJ. AS1411 alters the localization of a complex containing protein arginine methyltransferase 5 and nucleolin. Cancer Res. 2007; 67:10491–10500. [PubMed: 17974993]
36. Kang WJ, Ko MH, Lee DS, Kim S. Bioimaging of geographically adjacent proteins in a single cell by quantum dot-based fluorescent resonance energy transfer. Proteomics Clin. Appl. 2009; 3:1383–1388. [PubMed: 21136958]
37. Cai W, Chen X. Multimodality molecular imaging of tumor angiogenesis. J. Nucl. Med. 2008; 49 Suppl 2:113S–128S. [PubMed: 18523069]
38. Cai W, Shin DW, Chen K, Gheysens O, Cao Q, Wang SX, Gambhir SS, Chen X. Peptide-labeled near-infrared quantum dots for imaging tumor vasculature in living subjects. Nano Lett. 2006; 6:669–676. [PubMed: 16608262]
39. Ko MH, Kim S, Kang WJ, Lee JH, Kang H, Moon SH, Hwang do W, Ko HY, Lee DS. In vitro derby imaging of cancer biomarkers using quantum dots. Small. 2009; 5:1207–1212. [PubMed: 19235198]
40. Lee KY, Kang H, Ryu SH, Lee DS, Lee JH, Kim S. Bioimaging of nucleolin aptamer-containing 5-(N-benzylcarboxyamide)-2'-deoxyuridine more capable of specific binding to targets in cancer cells. J. Biomed. Biotechnol. 2010:168306. [PubMed: 20204158]
41. Singh R, Bandyopadhyay D. MUC1: a target molecule for cancer therapy. Cancer Biol. Ther. 2007; 6:481–486. [PubMed: 18027437]
42. Taylor-Papadimitriou J, Burchell J, Miles DW, Dalziel M. MUC1 and cancer. Biochim. Biophys. Acta. 1999; 1455:301–313. [PubMed: 10571020]
43. Savla R, Taratula O, Garbuzenko O, Minko T. Tumor targeted quantum dot-mucin 1 aptamer-doxorubicin conjugate for imaging and treatment of cancer. J. Control. Release. 2011 Epub.
44. Zhang J, Jia X, Lv XJ, Deng YL, Xie HY. Fluorescent quantum dot-labeled aptamer bioprobes specifically targeting mouse liver cancer cells. Talanta. 2010; 81:505–509. [PubMed: 20188954]
45. Cui ZQ, Ren Q, Wei HP, Chen Z, Deng JY, Zhang ZP, Zhang XE. Quantum dot-aptamer nanoprobes for recognizing and labeling influenza A virus particles. Nanoscale. 2011 Epub.
46. Wang W, Wu WY, Zhong X, Miao Q, Zhu JJ. Aptamer-based PDMS-gold nanoparticle composite as a platform for visual detection of biomolecules with silver enhancement. Biosens. Bioelectron. 2011; 26:3110–3114. [PubMed: 21227677]
47. Smith JE, Medley CD, Tang Z, Shangguan D, Lofton C, Tan W. Aptamer-conjugated nanoparticles for the collection and detection of multiple cancer cells. Anal. Chem. 2007; 79:3075–3082. [PubMed: 17348633]
48. Elenko MP, Szostak JW, van Oijen AM. Single-molecule imaging of an in vitro-evolved RNA aptamer reveals homogeneous ligand binding kinetics. J. Am. Chem. Soc. 2009; 131:9866–9867. [PubMed: 19572753]
49. Mallikaratchy P, Tang Z, Kwame S, Meng L, Shangguan D, Tan W. Aptamer directly evolved from live cells recognizes membrane bound immunoglobin heavy mu chain in Burkitt's lymphoma cells. Mol. Cell. Proteomics. 2007; 6:2230–2238. [PubMed: 17875608]
50. Shi H, Tang Z, Kim Y, Nie H, Huang YF, He X, Deng K, Wang K, Tan W. In vivo fluorescence imaging of tumors using molecular aptamers generated by cell-SELEX. Chem. Asian J. 2010; 5:2209–2213. [PubMed: 20806314]
51. Constantin TP, Silva GL, Robertson KL, Hamilton TP, Fague K, Waggoner AS, Armitage BA. Synthesis of new fluorogenic cyanine dyes and incorporation into RNA fluoromodules. Org. Lett. 2008; 10:1561–1564. [PubMed: 18338898]
52. Weissleder R, Mahmood U. Molecular imaging. Radiology. 2001; 219:316–333. [PubMed: 11323453]
53. Yang Y, Hong H, Zhang Y, Cai W. Molecular imaging of proteases in cancer. Cancer Growth Metastasis. 2009; 2:13–27. [PubMed: 20234801]
54. Stefflova K, Chen J, Zheng G. Using molecular beacons for cancer imaging and treatment. Front. Biosci. 2007; 12:4709–4721. [PubMed: 17485407]

55. Wang K, Tang Z, Yang CJ, Kim Y, Fang X, Li W, Wu Y, Medley CD, Cao Z, Li J, Colon P, Lin H, Tan W. Molecular engineering of DNA: molecular beacons. Angew. Chem. Int. Ed. Engl. 2009; 48:856–870. [PubMed: 19065690]
56. Tsien RY. Building and breeding molecules to spy on cells and tumors. FEBS Lett. 2005; 579:927–932. [PubMed: 15680976]
57. McIntyre JO, Matrisian LM. Molecular imaging of proteolytic activity in cancer. J. Cell Biochem. 2003; 90:1087–1097. [PubMed: 14635184]
58. Tok J, Lai J, Leung T, Li SF. Molecular aptamer beacon for myotonic dystrophy kinase-related Cdc42-binding kinase alpha. Talanta. 2010; 81:732–736. [PubMed: 20188990]
59. Shi H, He X, Wang K, Wu X, Ye X, Guo Q, Tan W, Qing Z, Yang X, Zhou B. Activatable aptamer probe for contrast-enhanced in vivo cancer imaging based on cell membrane protein-triggered conformation alteration. Proc. Natl. Acad. Sci. USA. 2011; 108:3900–3905. [PubMed: 21368158]
60. Winter PM, Caruthers SD, Wickline SA, Lanza GM. Molecular imaging by MRI. Curr. Cardiol. Rep. 2006; 8:65–69. [PubMed: 16507239]
61. Zhang Z, Nair SA, McMurry TJ. Gadolinium meets medicinal chemistry: MRI contrast agent development. Curr. Med. Chem. 2005; 12:751–778. [PubMed: 15853710]
62. Pathak AP, Gimi B, Glunde K, Ackerstaff E, Artemov D, Bhujwalla ZM. Molecular and functional imaging of cancer: Advances in MRI and MRS. Methods Enzymol. 2004; 386:3–60. [PubMed: 15120245]
63. Yigit MV, Mazumdar D, Kim HK, Lee JH, Odintsov B, Lu Y. Smart "turn-on" magnetic resonance contrast agents based on aptamer-functionalized superparamagnetic iron oxide nanoparticles. Chembiochem. 2007; 8:1675–1678. [PubMed: 17696177]
64. Xu W, Lu Y. A smart magnetic resonance imaging contrast agent responsive to adenosine based on a DNA aptamer-conjugated gadolinium complex. Chem. Commun. 2011; 47:4998–5000.
65. Tanaka K, Kitamura N, Chujo Y. Properties of superparamagnetic iron oxide nanoparticles assembled on nucleic acids. Nucleic Acids Symp. Ser. (Oxf). 2008:693–694.
66. Yigit MV, Mazumdar D, Lu Y. MRI detection of thrombin with aptamer functionalized superparamagnetic iron oxide nanoparticles. Bioconjug. Chem. 2008; 19:412–417. [PubMed: 18173225]
67. Paul D, Samuel SM, Maulik N. Mesenchymal stem cell: present challenges and prospective cellular cardiomyoplasty approaches for myocardial regeneration. Antioxid. Redox. Signal. 2009; 11:1841–1855. [PubMed: 19260767]
68. Pittenger MF, Martin BJ. Mesenchymal stem cells and their potential as cardiac therapeutics. Circ. Res. 2004; 95:9–20. [PubMed: 15242981]
69. Schafer R, Wiskirchen J, Guo K, Neumann B, Kehlbach R, Pintaske J, Voth V, Walker T, Scheule AM, Greiner TO, Hermanutz-Klein U, Claussen CD, Northoff H, Ziemer G, Wendel HP. Aptamer-based isolation and subsequent imaging of mesenchymal stem cells in ischemic myocard by magnetic resonance imaging. Rofo. 2007; 179:1009–1015. [PubMed: 17879173]
70. Wang AZ, Bagalkot V, Vasilliou CC, Gu F, Alexis F, Zhang L, Shaikh M, Yuet K, Cima MJ, Langer R, Kantoff PW, Bander NH, Jon S, Farokhzad OC. Superparamagnetic iron oxide nanoparticle-aptamer bioconjugates for combined prostate cancer imaging and therapy. ChemMedChem. 2008; 3:1311–1315. [PubMed: 18613203]
71. Yu MK, Kim D, Lee IH, So JS, Jeong YY, Jon S. Image-guided prostate cancer therapy using aptamer-functionalized thermally cross-linked superparamagnetic iron oxide nanoparticles. Small. 2011 Epub.
72. Nair BG, Nagaoka Y, Morimoto H, Yoshida Y, Maekawa T, Kumar DS. Aptamer conjugated magnetic nanoparticles as nanosurgeons. Nanotechnology. 2010; 21:455102. [PubMed: 20947949]
73. Jakobsen JA. Ultrasound contrast agents: clinical applications. Eur. Radiol. 2001; 11:1329–1337. [PubMed: 11519539]
74. Kaufmann BA, Lindner JR. Molecular imaging with targeted contrast ultrasound. Curr. Opin. Biotechnol. 2007; 18:11–16. [PubMed: 17241779]
75. Wang CH, Huang YF, Yeh CK. Aptamer-conjugated nanobubbles for targeted ultrasound molecular imaging. Langmuir. 2011; 27:6971–6976. [PubMed: 21553884]

76. Maul TM, Dudgeon DD, Beste MT, Hammer DA, Lazo JS, Villanueva FS, Wagner WR. Optimization of ultrasound contrast agents with computational models to improve selection of ligands and binding strength. Biotechnol. Bioeng. 2010; 107:854–864. [PubMed: 20665479]
77. Younes CK, Boisgard R, Tavitian B. Labelled oligonucleotides as radiopharmaceuticals: pitfalls, problems and perspectives. Curr. Pharm. Des. 2002; 8:1451–1466. [PubMed: 12052206]
78. Lucignani G. Aptamers and in-beam PET for advanced diagnosis and therapy optimisation. Eur. J. Nucl. Med. Mol. Imaging. 2006; 33:1095–1097. [PubMed: 16896657]
79. Perkins AC, Missailidis S. Radiolabelled aptamers for tumour imaging and therapy. Q. J. Nucl. Med. Mol. Imaging. 2007; 51:292–296. [PubMed: 17464274]
80. Peremans K, Cornelissen B, Van Den Bossche B, Audenaert K, Van de Wiele C. A review of small animal imaging planar and pinhole spect Gamma camera imaging. Vet. Radiol. Ultrasound. 2005; 46:162–170. [PubMed: 15869162]
81. Charlton J, Sennello J, Smith D. In vivo imaging of inflammation using an aptamer inhibitor of human neutrophil elastase. Chem. Biol. 1997; 4:809–816. [PubMed: 9384527]
82. Doring G. The role of neutrophil elastase in chronic inflammation. Am. J. Respir. Crit. Care Med. 1994; 150:S114–S117. [PubMed: 7952645]
83. Charlton J, Kirschenheuter GP, Smith D. Highly potent irreversible inhibitors of neutrophil elastase generated by selection from a randomized DNA-valine phosphonate library. Biochemistry. 1997; 36:3018–3026. [PubMed: 9062133]
84. Orend G. Potential oncogenic action of tenascin-C in tumorigenesis. Int. J. Biochem. Cell Biol. 2005; 37:1066–1083. [PubMed: 15743679]
85. Orend G, Chiquet-Ehrismann R. Tenascin-C induced signaling in cancer. Cancer Lett. 2006; 244:143–163. [PubMed: 16632194]
86. Hicke BJ, Stephens AW, Gould T, Chang YF, Lynott CK, Heil J, Borkowski S, Hilger CS, Cook G, Warren S, Schmidt PG. Tumor targeting by an aptamer. J. Nucl. Med. 2006; 47:668–678. [PubMed: 16595502]
87. Borbas KE, Ferreira CS, Perkins A, Bruce JI, Missailidis S. Design and synthesis of mono- and multimeric targeted radiopharmaceuticals based on novel cyclen ligands coupled to anti-MUC1 aptamers for the diagnostic imaging and targeted radiotherapy of cancer. Bioconjug. Chem. 2007; 18:1205–1212. [PubMed: 17583928]
88. Liu S, Edwards DS. ^{99m}Tc-labeled small peptides as diagnostic radiopharmaceuticals. Chem. Rev. 1999; 99:2235–2268. [PubMed: 11749481]
89. Pieve CD, Perkins AC, Missailidis S. Anti-MUC1 aptamers: radiolabelling with ^{99m}Tc and biodistribution in MCF-7 tumour-bearing mice. Nucl. Med. Biol. 2009; 36:703–710. [PubMed: 19647177]
90. Ter-Pogossian MM, Phelps ME, Hoffman EJ, Mullani NA. A positron-emission transaxial tomograph for nuclear imaging (PETT). Radiology. 1975; 114:89–98. [PubMed: 1208874]
91. Phelps ME, Hoffman EJ, Mullani NA, Ter-Pogossian MM. Application of annihilation coincidence detection to transaxial reconstruction tomography. J. Nucl. Med. 1975; 16:210–224. [PubMed: 1113170]
92. Gambhir SS. Molecular imaging of cancer with positron emission tomography. Nat. Rev. Cancer. 2002; 2:683–693. [PubMed: 12209157]
93. Chatziioannou AF. Instrumentation for molecular imaging in preclinical research: Micro-PET and Micro-SPECT. Proc. Am. Thorac. Soc. 2005; 2:533–536. 510-511. [PubMed: 16352760]
94. Stickel JR, Qi J, Cherry SR. Fabrication and characterization of a 0.5-mm lutetium oxyorthosilicate detector array for high-resolution PET applications. J. Nucl. Med. 2007; 48:115–121. [PubMed: 17204707]
95. Rockey WM, Huang L, Kloepping KC, Baumhover NJ, Giangrande PH, Schultz MK. Synthesis and radiolabeling of chelator-RNA aptamer bioconjugates with copper-64 for targeted molecular imaging. Bioorg. Med. Chem. 2011 Epub.
96. Chen LQ, Xiao SJ, Peng L, Wu T, Ling J, Li YF, Huang CZ. Aptamer-based silver nanoparticles used for intracellular protein imaging and single nanoparticle spectral analysis. J. Phys. Chem. B. 2010; 114:3655–3659. [PubMed: 20112983]

97. Kim NH, Lee SJ, Moskovits M. Aptamer-mediated surface-enhanced Raman spectroscopy intensity amplification. Nano Lett. 2010; 10:4181–4185. [PubMed: 20863079]

98. Mortele KJ, McTavish J, Ros PR. Current techniques of computed tomography. Helical CT, multidetector CT, and 3D reconstruction. Clin. Liver Dis. 2002; 6:29–52. [PubMed: 11933594]

99. Nelson RC, Chezmar JL, Peterson JE, Bernardino ME. Contrast-enhanced CT of the liver and spleen: comparison of ionic and nonionic contrast agents. AJR Am. J. Roentgenol. 1989; 153:973–976. [PubMed: 2801447]

100. Remy-Jardin M, Bahepar J, Lafitte JJ, Dequiedt P, Ertzbischoff O, Bruzzi J, Delannoy-Deken V, Duhamel A, Remy J. Multi-detector row CT angiography of pulmonary circulation with gadolinium-based contrast agents: prospective evaluation in 60 patients. Radiology. 2006; 238:1022–1035. [PubMed: 16505397]

101. Wisner ER, Theon A, Griffey SM, McIntire GL. Long-term effect of irradiation on lymph node uptake of interstitially delivered nanoparticulate contrast media. Invest. Radiol. 2000; 35:199–204. [PubMed: 10719830]

102. Rabin O, Manuel Perez J, Grimm J, Wojtkiewicz G, Weissleder R. An X-ray computed tomography imaging agent based on long-circulating bismuth sulphide nanoparticles. Nat. Mater. 2006; 5:118–122. [PubMed: 16444262]

103. Hyafil F, Cornily JC, Feig JE, Gordon R, Vucic E, Amirbekian V, Fisher EA, Fuster V, Feldman LJ, Fayad ZA. Noninvasive detection of macrophages using a nanoparticulate contrast agent for computed tomography. Nat. Med. 2007; 13:636–641. [PubMed: 17417649]

104. Cai W, Chen X. Nanoplatforms for targeted molecular imaging in living subjects. Small. 2007; 3:1840–1854. [PubMed: 17943716]

105. Kim D, Jeong YY, Jon S. A drug-loaded aptamer-gold nanoparticle bioconjugate for combined CT imaging and therapy of prostate cancer. ACS Nano. 2010; 4:3689–3696. [PubMed: 20550178]

106. Homola J. Surface plasmon resonance sensors for detection of chemical and biological species. Chem. Rev. 2008; 108:462–493. [PubMed: 18229953]

107. Piliarik M, Vaisocherova H, Homola J. Surface plasmon resonance biosensing. Methods Mol. Biol. 2009; 503:65–88. [PubMed: 19151937]

108. Li Y, Lee HJ, Corn RM. Fabrication and characterization of RNA aptamer microarrays for the study of protein-aptamer interactions with SPR imaging. Nucleic Acids Res. 2006; 34:6416–6424. [PubMed: 17130155]

109. Li Y, Lee HJ, Corn RM. Detection of protein biomarkers using RNA aptamer microarrays and enzymatically amplified surface plasmon resonance imaging. Anal. Chem. 2007; 79:1082–1088. [PubMed: 17263339]

110. Seefeld TH, Zhou WJ, Corn RM. Rapid microarray detection of DNA and proteins in microliter volumes with surface plasmon resonance imaging measurements. Langmuir. 2011; 27:6534–6540. [PubMed: 21488682]

111. Wang Z, Wilkop T, Xu D, Dong Y, Ma G, Cheng Q. Surface plasmon resonance imaging for affinity analysis of aptamer-protein interactions with PDMS microfluidic chips. Anal. Bioanal. Chem. 2007; 389:819–825. [PubMed: 17673982]

112. Lautner G, Balogh Z, Bardoczy V, Meszaros T, Gyurcsanyi RE. Aptamer-based biochips for label-free detection of plant virus coat proteins by SPR imaging. Analyst. 2010; 135:918–926. [PubMed: 20419239]

113. Hwang do W, Ko HY, Lee JH, Kang H, Ryu SH, Song IC, Lee DS, Kim S. A nucleolin-targeted multimodal nanoparticle imaging probe for tracking cancer cells using an aptamer. J. Nucl. Med. 2010; 51:98–105. [PubMed: 20008986]

114. Thiel KW, Giangrande PH. Therapeutic applications of DNA and RNA aptamers. Oligonucleotides. 2009; 19:209–222. [PubMed: 19653880]

115. Fang X, Tan W. Aptamers generated from cell-SELEX for molecular medicine: a chemical biology approach. Acc. Chem. Res. 2010; 43:48–57. [PubMed: 19751057]

116. Mayer G. The chemical biology of aptamers. Angew. Chem. Int. Ed. Engl. 2009; 48:2672–2689. [PubMed: 19319884]

117. Rudin M, Weissleder R. Molecular imaging in drug discovery and development. Nat. Rev. Drug Discov. 2003; 2:123–131. [PubMed: 12563303]
118. Cai W, Rao J, Gambhir SS, Chen X. How molecular imaging is speeding up anti-angiogenic drug development. Mol. Cancer Ther. 2006; 5:2624–2633. [PubMed: 17121909]
119. Frangioni JV. *In vivo* near-infrared fluorescence imaging. Curr. Opin. Chem. Biol. 2003; 7:626–634. [PubMed: 14580568]
120. Cai W, Chen K, Li ZB, Gambhir SS, Chen X. Dual-function probe for PET and near-infrared fluorescence imaging of tumor vasculature. J. Nucl. Med. 2007; 48:1862–1870. [PubMed: 17942800]
121. Chen K, Li ZB, Wang H, Cai W, Chen X. Dual-modality optical and positron emission tomography imaging of vascular endothelial growth factor receptor on tumor vasculature using quantum dots. Eur. J. Nucl. Med. Mol. Imaging. 2008; 35:2235–2244. [PubMed: 18566815]
122. Lee HY, Li Z, Chen K, Hsu AR, Xu C, Xie J, Sun S, Chen X. PET/MRI dual-modality tumor imaging using arginine-glycine-aspartic (RGD)-conjugated radiolabeled iron oxide nanoparticles. J. Nucl. Med. 2008; 49:1371–1379. [PubMed: 18632815]
123. Xie J, Chen K, Huang J, Lee S, Wang J, Gao J, Li X, Chen X. PET/NIRF/MRI triple functional iron oxide nanoparticles. Biomaterials. 2010; 31:3016–3022. [PubMed: 20092887]
124. Hong H, Zhang Y, Sun J, Cai W. Molecular imaging and therapy of cancer with radiolabeled nanoparticles. Nano Today. 2009; 4:399–413. [PubMed: 20161038]
125. Missailidis S, Hardy A. Aptamers as inhibitors of target proteins. Expert Opin. Ther. Pat. 2009; 19:1073–1082. [PubMed: 19514954]
126. Lee JH, Yigit MV, Mazumdar D, Lu Y. Molecular diagnostic and drug delivery agents based on aptamer-nanomaterial conjugates. Adv. Drug Deliv. Rev. 2010; 62:592–605. [PubMed: 20338204]

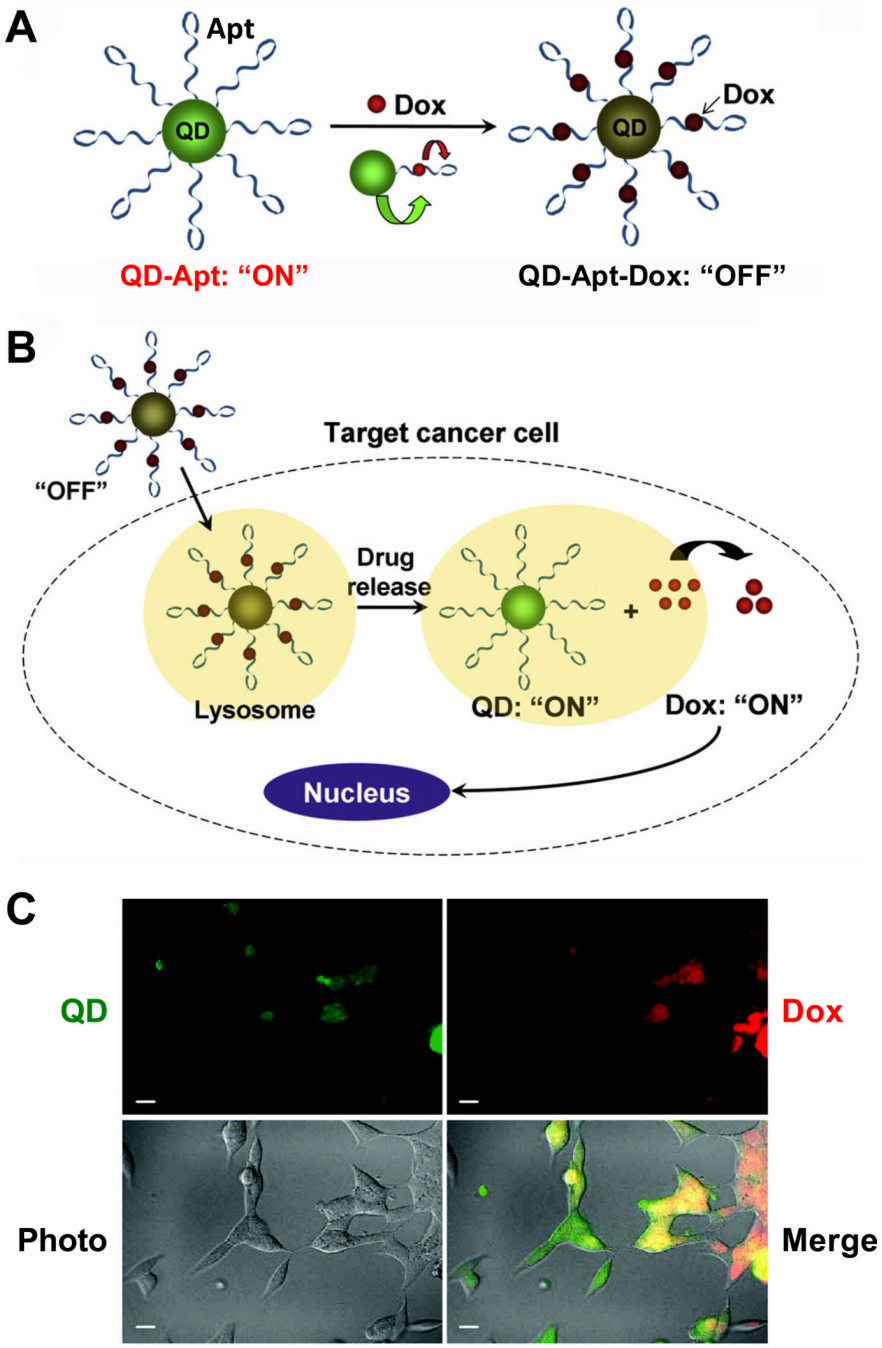

Fig. 1.

A QD-Apt-Dox conjugate. **A.** QD-Apt-Dox is initially "off" as the fluorescence of QD is transferred to Dox and the fluorescence of Dox is quenched by the aptamer, both by fluorescence resonance energy transfer. **B.** Once QD-Apt-Dox is inside cancer cells, Dox is gradually released from the conjugate and the fluorescence of QD is recovered. **C.** Microscopy images of PSMA-positive cells after incubation with QD-Apt-Dox. QD and Dox are shown in green and red, respectively. Scale bar: 20 μm. Adapted from [33,126].

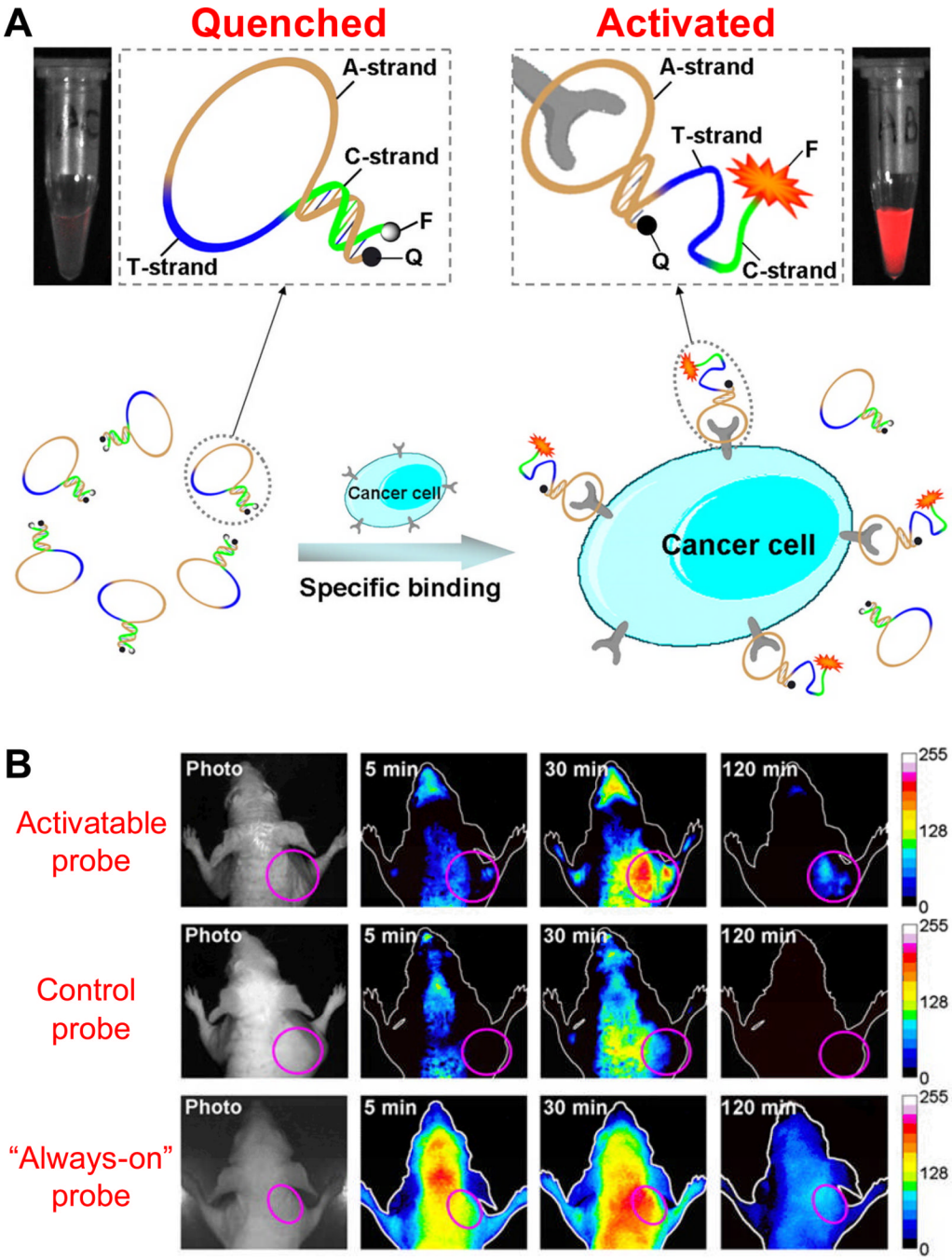

Fig. 2.

Fluorescence imaging with an aptamer-based activatable probe. **A.** A schematic representation of the imaging strategy based on cell membrane protein-triggered conformation alteration. The probe is consisted of three fragments: a cancer-targeted aptamer sequence (A-strand), a poly-T linker (T-strand), and a short DNA sequence (C-strand) complementary to a part of the A-strand, with a fluorophore (F) and a quencher (Q) attached at either terminus. When no target is present, the probe is hairpin-structured with quenched fluorescence. When the probe binds to targeted cancer cells, its conformation is altered which results in enhanced fluorescence signal. **B.** Serial in vivo fluorescence imaging of tumor-bearing mice after intravenous injection of the activatable probe, a control probe,

or an “always-on” probe. The circles in the images denote the tumor sites. Adapted from [59].

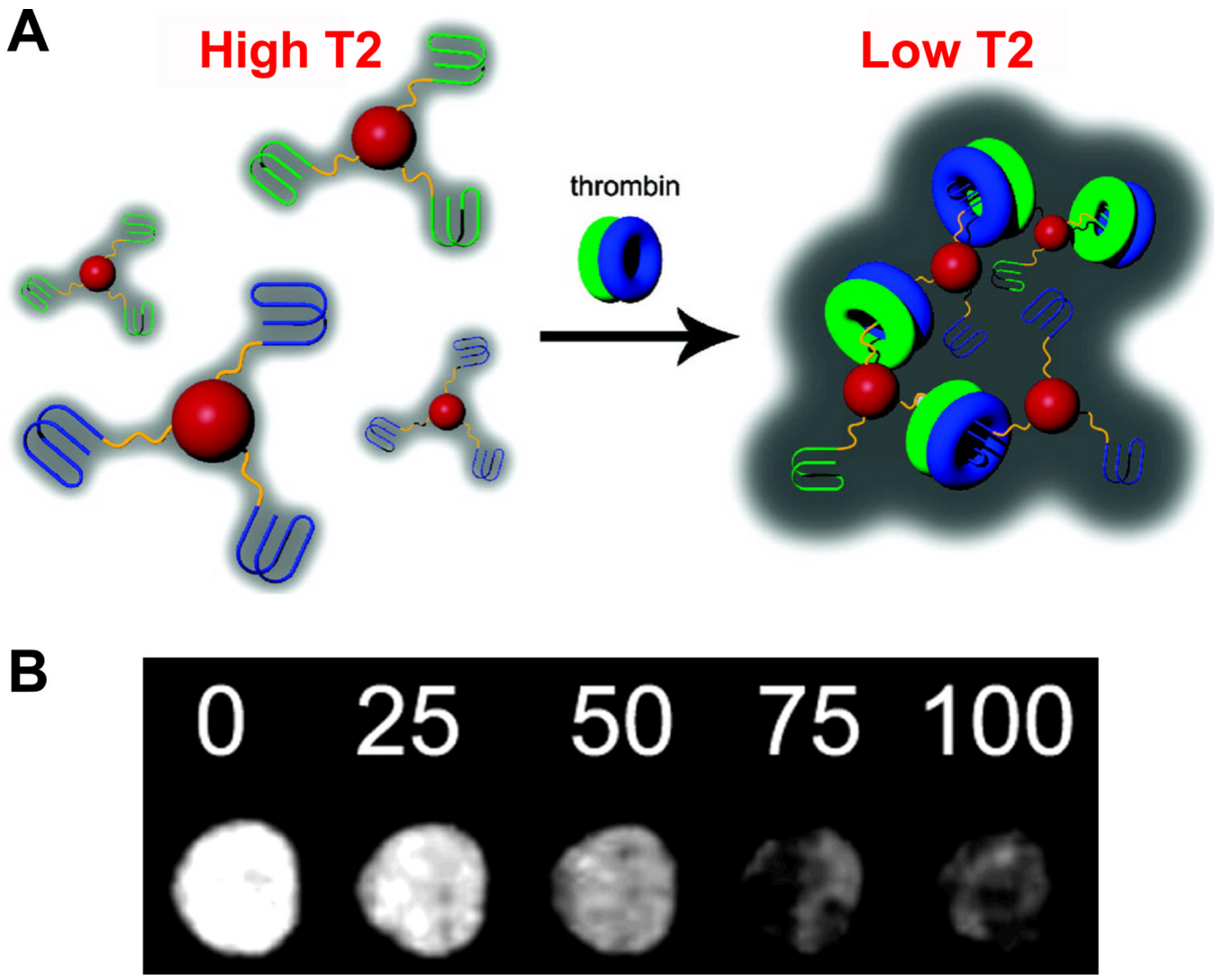

Fig. 3.

Molecular MRI with an aptamer-based probe. **A.** The iron oxide nanoparticles (red spheres) were modified with DNA aptamers that binds to fibrinogen-recognition exosite of thrombin (blue lines) or heparin-binding exosite of thrombin (green lines). Addition of thrombin consisting of both fibrinogen (blue donuts) and heparin (green donuts) exosites results in nanoparticle aggregation, which leads to reduced T2 relaxation time. **B.** T2-weighted magnetic resonance images of 1:1 nanoparticle mixture in the presence of various concentrations of thrombin (in the unit of nanomolar). Adapted from [66].

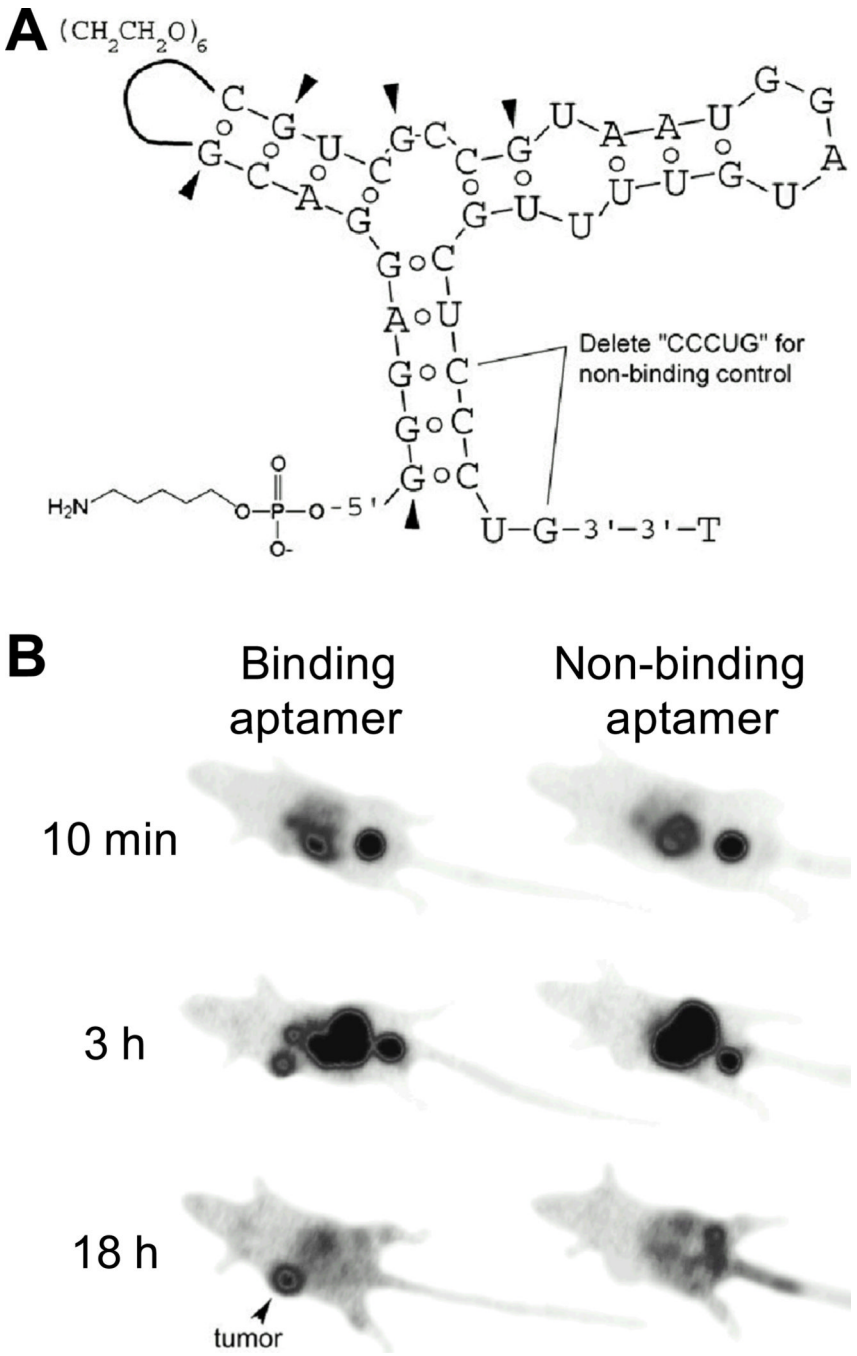

Fig. 4.

SPECT imaging with a ^{99m}Tc-labeled aptamer. **A.** Structure of the aptamer. Pyrimidines are 2'-F and purines are 2'-OMe, except at arrowheads, where purines remain 2'-OH. The non-binding control aptamer has 5-nucleotide internal deletion. **B.** Serial gamma camera imaging of tumors (arrowheads) after intravenous injection of ^{99m}Tc-labeled aptamers. Adapted from [86].

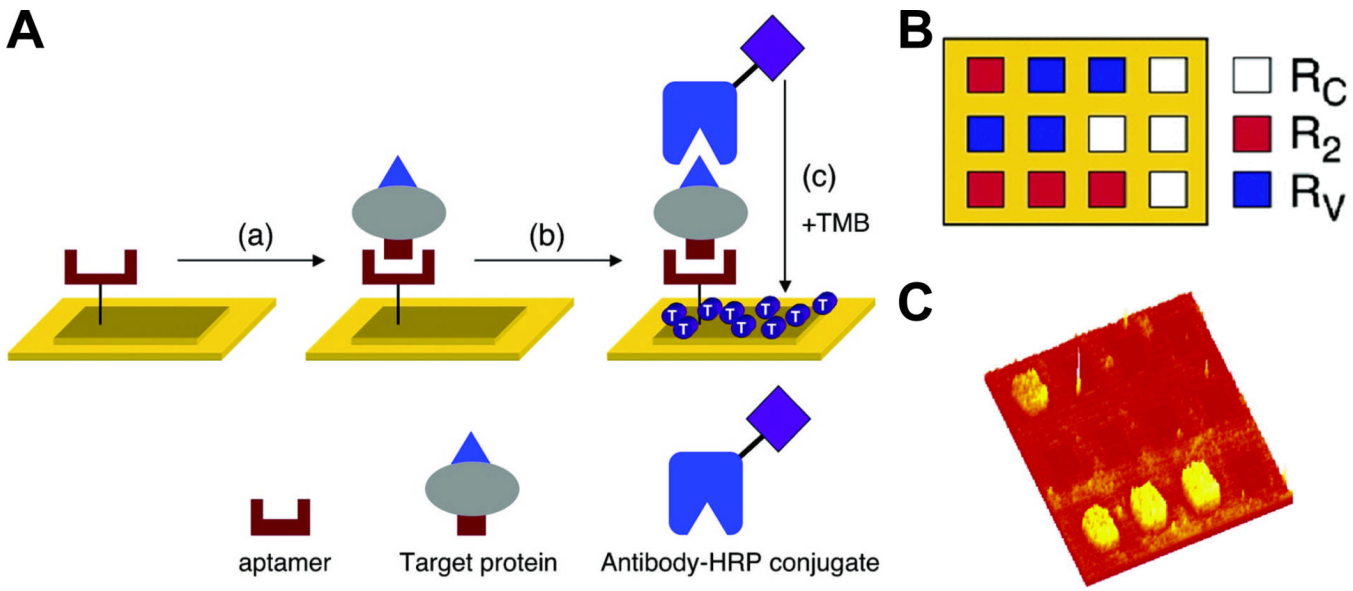

Fig. 5.

Detection of protein biomarkers using RNA aptamer microarrays and enzymatically amplified surface plasmon resonance (SPR) imaging. **A.** In step a, the target protein binds to the surface-immobilized aptamer. In step b, a horseradish peroxidase (HRP)-conjugated antibody to the target protein is introduced to create a surface aptamer-protein-antibody sandwich structure. In step c, this surface is exposed to the substrate 3,3',5,5'-tetramethylbenzidine (TMB), which reacts with HRP to form a dark blue precipitate on the array elements containing the complex, detectable by SPR imaging. **B.** Pattern of the three-component RNA microarray for detection, each color represents the use of a RNA aptamer against a different target. **C.** A SPR difference image obtained for R_2. Adapted from [109].

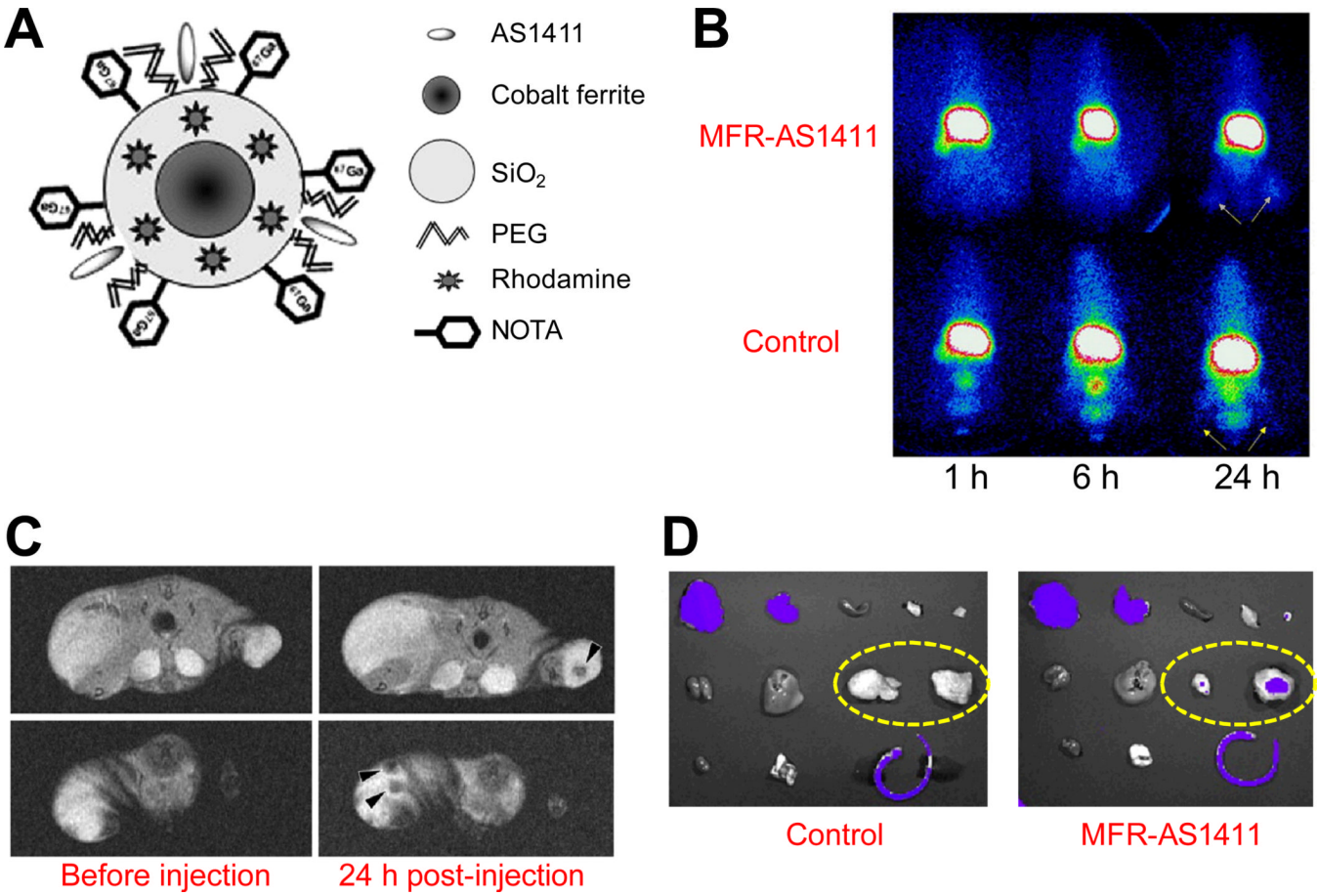

Fig. 6.

Multimodality imaging with an aptamer-based probe. **A.** A schematic illustration of the probe MFR-AS1411. **B.** Serial gamma camera imaging of tumor-bearing mice after intravenous injection of MFR-AS1411 or a control probe which contains a mutated aptamer. Arrows indicate tumors. **C.** Magnetic resonance images of tumor-bearing mice before and after injection of MFR-AS1411. Dark signal intensities at tumor sites (arrowheads) were detected in mice injected with MFR-AS14110. **D.** Ex vivo fluorescence imaging of major organs. Dashed ovals indicate the tumors. Adapted from [113].

Table 1

A tabulated summary of aptamer-based molecular imaging.

Target	Image tag	Imaging technique	In vivo study?	Ref.
Integrin $\alpha_v\beta_3$	Cy5	Fluorescence	No	[21]
Angiogenin	Cy5	Fluorescence	No	[24]
PSMA	Cy5, quantum dot	Fluorescence	No	[27,30,33]
Nucleolin	Cy3, quantum dot	Fluorescence	No	[36,39,40]
MUC1	Quantum dot	Fluorescence	Yes	[43]
Hepatoma cells	Quantum dot	Fluorescence	No	[44]
Hemagglutinin	Quantum dot	Fluorescence	No	[45]
Cells	Magnetic and fluorescent NPs	Fluorescence	No	[47]
Guanosine triphosphate	Tetramethylrhodamine	Fluorescence	No	[48]
Ramos cells	Cy5	Fluorescence	Yes	[50]
MRCK	Fluorophore-quencher pair	Fluorescence	No	[58]
Cancer cells	Fluorophore-quencher pair	Fluorescence	Yes	[59]
Adenosine	Gadolinium, iron oxide NPs	MRI	No	[63,64]
Thrombin	Iron oxide NPs	MRI	No	[66]
MSC	SPIO	MRI	Yes	[69]
PSMA	SPIO	MRI	No	[70]
PSMA	SPIO	MRI	Yes	[71]
Leukemia cells	Nanobubbles	Ultrasound	No	[75]
Elastase	^{99m}Tc	SPECT	Yes	[81]
Tenascin-C	Rhodamine red/^{99m}Tc/^{111}In	Fluorescence/SPECT	Yes	[86]
MUC1	^{99m}Tc	Autoradiography	Yes	[87]
Prion protein	Silver NPs	Dark-field light scattering	No	[96]
Adenosine	Gold NPs	SERS	No	[97]
PSMA	Gold NPs	CT	No	[105]
Nucleolin	Cobalt-ferrite NPs/rhodamine/^{67}Ga	MRI/fluorescence/SPECT	Yes	[113]